Recent Results from TRISTAN

Stephen L. Olsen*
Department of Physics and Astronomy, University of Rochester, Rochester, NY 14627, USA

ABSTRACT

We report on recent measurements of lepton and quark cross sections and asymmetries at TRISTAN. We find that the application of new methods for computing radiative corrections resolves the long-standing discrepancy between the measured values of the total cross section for annihilation into hadrons and Standard Model predictions. The differential cross sections for $e^+e^- \longrightarrow \mu^+\mu^-$ and $\tau^+\tau^-$ exhibit forward-backward charge asymmetries that are consistent with the Standard Model, but total cross sections that are only marginally consistent with the model's predictions. In addition, we describe an analysis of hadron production in quasi-real photon-photon collisions. An excess of high transverse momentum hadrons, beyond expectations of the Vector-Dominance and Quark-Parton models, is attributed to hard scattering between the photons' hadronic constituents.

1. Electro-Weak Cross Sections and Asymmetries

In the Standard Model (SM), the lowest-order cross section for the electro-weak process $e^+e^- \longrightarrow f\bar{f}$ ($f\bar{f} = \mu^+\mu^-,\ \tau^+\tau^-$, or $q\bar{q}$) is given by

$$\frac{d\sigma}{d\Omega} = \frac{\alpha^2}{4s} R_{ff}(1 + \cos^2\theta + \frac{8}{3} A_{ff}\cos\theta), \tag{1}$$

where R_{ff}, the ratio of the total cross section to the lowest-order QED expression for mu-pair production, is

$$R_{ff} = q_f^2 + 8v_e v_f \mathrm{Re}(\chi) + 16\left(v_e^2 + a_e^2\right)\left(v_f^2 + a_f^2\right)\chi^2, \tag{2}$$

and the forward-backward charge asymmetry A_{ff} is

$$A_{ff} = \frac{1}{R_{ff}}\left(6a_e a_f \mathrm{Re}(\chi) + 48 v_e v_f a_e a_f \chi^2\right). \tag{3}$$

Here q_f is the final-state fermion's electric charge in units of the electron charge, and v and a are the vector- and axial-vector couplings of the fermions to the Z°. The contribution from the Z° pole is contained in χ, where

$$\chi = \frac{1}{16\sin^2\theta_W\cos^2\theta_W}\cdot\frac{s}{s - M_Z^2 + i\Gamma_Z M_Z}. \tag{4}$$

*Representing the AMY, TOPAZ and VENUS Collaborations.

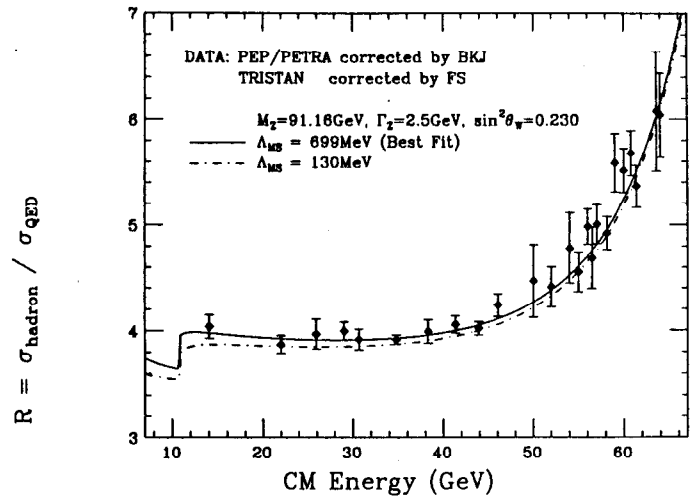

Figure 1: Values of R_{had} from PEP, PETRA and TRISTAN corrected by the BKJ/FS technique. The solid curve is a fit to the SM, which gives $\Lambda_{\overline{MS}} = 699$ MeV; the dashed line shows the SM expectation for $\Lambda_{\overline{MS}} = 130$ MeV.

In the TRISTAN energy region the effects of the Z° pole are comparable to those of the virtual photon. As a result, the interference between the two is large and there are large forward-backward asymmetries.

The experimentally measured cross sections and asymmetries are expected to differ from the above-noted predictions because of the effects of higher-order electroweak and, for the case of $f\overline{f} = q\overline{q}$ (i.e., quark-antiquark pairs), QCD processes. Traditionally, electroweak radiative corrections are applied to the data before extracting R and A; at TRISTAN these are calculated to $\mathcal{O}(\alpha^3)$ using the program of Fujimoto and Shimizu (FS).[1] Measurements at PEP and PETRA are corrected using the program of Behrends, Kleiss, and Jadach (BKJ).[2] The corrected data are compared to SM predictions for R_{qq} that include modifications due to higher order QCD corrections. QCD corrections to order α_s^3 are given in ref. 3.

1.1. $e^+e^- \longrightarrow$ Hadrons

While the SM predictions for the process $e^+e^- \longrightarrow q\overline{q} \longrightarrow hadrons$ (R_{had}) are, in principle, straightforward, historically the agreement with experimental measurements has been poor. For example, fits of SM predictions to R_{had} measurements from PEP and PETRA always produced values for $\Lambda_{\overline{MS}}$, the QCD scale parameter, around $\Lambda_{\overline{MS}} \sim 700$ MeV,[4] substantially higher than the Particle Data Group's "preferred" value of 130^{+110}_{-60} MeV.[5] In addition, the R_{had} values measured at TRISTAN were higher than expectations—a discrepancy that could not be accommodated by a higher $\Lambda_{\overline{MS}}$ value. At the time, the only way to get agreement with SM predictions was to take the mass of the Z°, which then was thought to be $M_Z \simeq 92.5$ GeV/c^2, to be around 88 GeV/c^2.[6] Subsequent measurements at Fermilab,[7] SLAC,[8] and LEP[9] indicate that, while M_Z is, in fact, lower, i.e. $M_Z = 91.16 \pm 0.03$ GeV/c^2, it is not low enough to get good agreement between the PEP/PETRA/TRISTAN measured values of R_{had} and SM predictions without large $\Lambda_{\overline{MS}}$ values, as can be seen in Fig. 1.

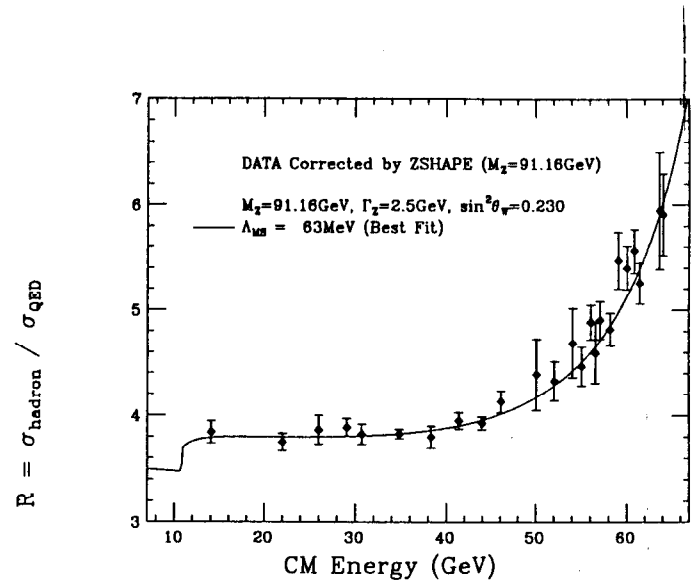

Figure 2: Values of R_{had} from PEP, PETRA and TRISTAN corrected using the ZSHAPE program. The solid curve is a fit to the SM, which gives $\Lambda_{\overline{MS}} = 63^{+173}_{-56}$MeV.

However, it was recently noted by Haidt[10] that if radiative corrections determined from the ZSHAPE program,[11] which was developed for LEP experiments, are used instead of the "traditional" FS or BKJ techniques for the PEP/PETRA/TRISTAN R_{had} measurements, the agreement with SM predictions, with a "reasonable" value for $\Lambda_{\overline{MS}}$ of ~70 MeV, is excellent, as can be seen in Fig. 2. The primary difference between the ZSHAPE calculation and that of FS and BKJ is in the relative treatment of the radiation-type diagrams (Fig. 3a) and vacuum-polarization-type diagrams (Fig. 3b). In the FS/BKJ approach, these terms are treated separately; in the ZSHAPE approach, the vacuum polarization diagrams, which have the effect of modifying the strength of the electric charge, are calculated first and the radiation processes are then calculated using the modified electric charge as indicated in Fig. 3c. (This is referred to as the "improved Born approximation.")

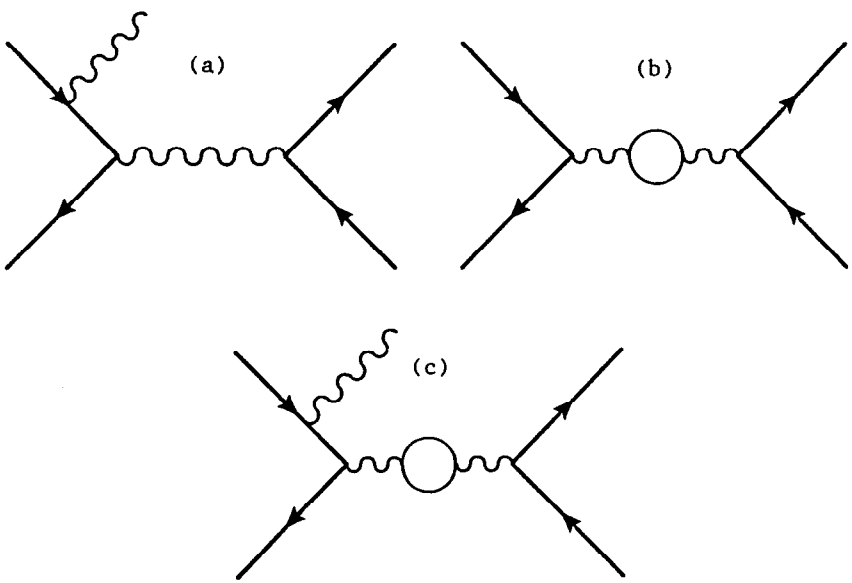

Figure 3: (a) The Feynman diagram for initial-state radiation. (b) A vacuum polarization diagram. (c) Initial-state radiation in the "improved Born approximation."

Roughly speaking, if we denote the correction due to radiation diagrams (Fig. 3a) as δ_{rad} and that due to vacuum polarization (Fig. 3b) as δ_{vac}, the FS/BKJ correction can be summarized as

$$1 + \delta^{tot}_{FS/BKJ} \simeq 1 + \delta_{rad} + \delta_{vac}, \tag{5}$$

whereas the ZSHAPE correction is

$$1 + \delta^{tot}_{ZSHAPE} \simeq (1 + \delta_{rad})(1 + \delta_{vac}), \tag{6}$$

with the essential difference between the two approaches lying in the extra cross term $\delta_{rad}\delta_{vac}$ that is included in ZSHAPE, but not in the FS/BKJ scheme. If we estimate the magnitudes of δ_{rad} and δ_{vac} as

$$\delta_{rad} \simeq \frac{\alpha(0)}{\pi} \ln \frac{s}{m_e^2} \ln \frac{E_{beam}}{E_{cut}} \simeq 0.25 \quad (\text{for} E_{cut} = 0.01 E_{beam}) \tag{7}$$

and

$$\delta_{vac} \simeq \left(\frac{\alpha(s)}{\alpha(0)}\right)^2 - 1 \simeq \left(\frac{137}{128}\right)^2 - 1 \simeq 0.14, \tag{8}$$

we find that the cross term is sizable, namely

$$\delta_{rad}\delta_{vac} \simeq 0.035, \tag{9}$$

certainly much larger than 1/137, the relative size one normally expects for higher order terms. Since ZSHAPE was created specifically for measurements near the Z° pole, it ignores quark masses and, thus, is not optimized for lower energy measurements. Nevertheless, it seems reasonable to expect that a properly optimized calculation will not change the essential features noted above and that the long-standing discrepancy between the R_{had} values measured at PEP/PETRA/TRISTAN and the SM predictions are resolved.

1.2. $e^+e^- \longrightarrow \mu^+\mu^-$ and $\tau^+\tau^-$

The SM predictions for the purely leptonic reactions $e^+e^- \longrightarrow \mu^+\mu^-$ and $\tau^+\tau^-$ are unambiguous. Preliminary results for the differential cross sections for $e^+e^- \longrightarrow \mu^+\mu^-$ and $\tau^+\tau^-$ from the AMY experiment are shown in Figs. 4a and 4b. Here the preponderance of events in the backward direction reflects the (negative) forward-backward asymmetry predicted by the SM. However, the total cross section for the $\mu^+\mu^-$ reaction appears to be somewhat lower than SM predictions, although the combined statistical and systematic errors make the effect less than compelling. Nevertheless, it is interesting to note that while no single experiment can make a statistically strong statement, most of the PEP/PETRA/TRISTAN measurements of $R_{\mu\mu}$ tend to be low, as can be seen in Fig. 5a (the scatter of the measurements of $R_{\tau\tau}$ are too large to make a statement one way or the other—see Fig. 5b). Here the data are corrected for higher order QED corrections using the FS/BKJ technique—the cross terms in the ZSHAPE method will, if anything, lower the measurements and increase the level of the discrepancy.

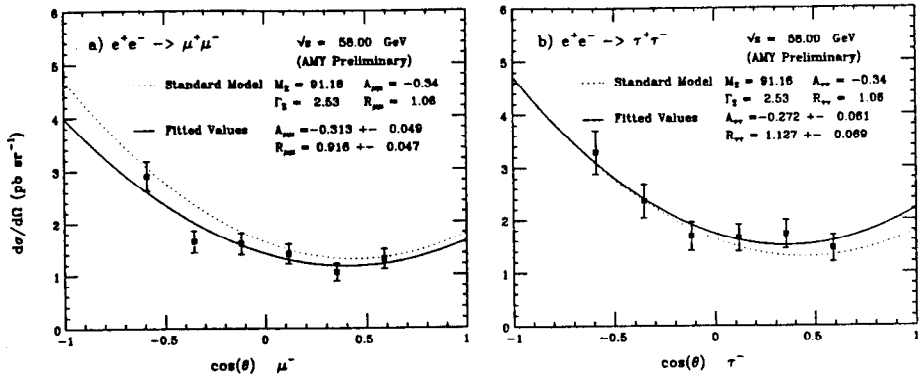

Figure 4: The measured differential cross section for $e^+e^- \longrightarrow \mu^+\mu^-$ (a) and $\tau^+\tau^-$ (b), from the AMY experiment at a cm energy of 58 GeV.

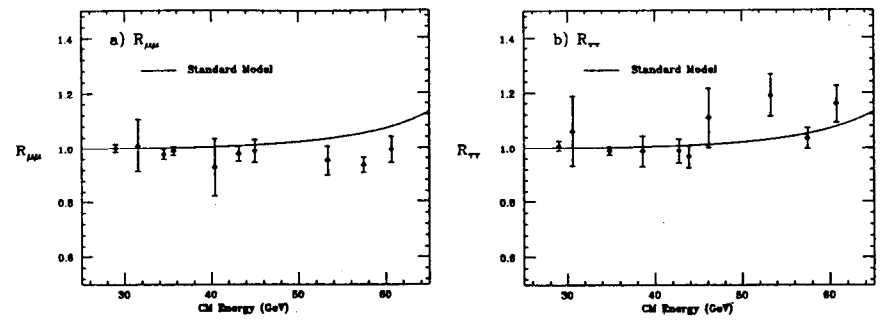

Figure 5: Values of $R_{\mu\mu}$ (a) and $R_{\tau\tau}$ (b) from PEP, PETRA and TRISTAN. The solid curve is the SM prediction.

1.3. Z′ Search

A major goal for the remainder of the TRISTAN experimental program is to measure R and A for mu-pair and tau-pair production with a statistical precision such that each of the three TRISTAN experiments can individually establish a $\sim$ 10% discrepancy with the SM, should it exist. The SM predictions for these processes contain no significant ambiguities, and, thus, a discrepancy with measurements would be a first indication for physics beyond the SM. At a summer institute such as this, it is instructive to examine possible modifications of the SM that such a discrepancy might imply.

In most of the proposed extensions to the theory, the $SU(3)_{color} \times SU(2)_{weak} \times U(1)_{em}$ structure of the SM originates from the breaking of a higher symmetry scheme. For example, in superstring-inspired E_6 models, the original E_6 symmetry is broken as

$$E_6 \longrightarrow SO(10) \times U(1)_\psi \tag{10}$$

with the subsequent breaking of the $SO(10)$ group as

$$SO(10) \longrightarrow SU(5) \times U(1)_\chi. \tag{11}$$

The SM comes from the breaking of the $SU(5)$ symmetry

$$SU(5) \longrightarrow SU(3)_{color} \times SU(2)_{weak} \times U(1)_{em}. \tag{12}$$

Each of the $U(1)$ groups that emerge from this breaking scheme gives rise to another neutral gauge boson (in addition to the Standard Model Z°); in the E_6 picture there

are two, the Z_ψ and Z_χ. In general, the observable neutral bosons will be mixtures of those from the original groups—we call the lighter one (i.e., the one whose effects we might hope to see at TRISTAN energies) the Z'; the heavier one is called the Z''. In terms of a mixing angle β,

$$\begin{pmatrix} Z' \\ Z'' \end{pmatrix} = \begin{pmatrix} \cos\beta & \sin\beta \\ -\sin\beta & \cos\beta \end{pmatrix} \begin{pmatrix} Z_\psi \\ Z_\chi \end{pmatrix}. \tag{13}$$

Models with different choices of β have been proposed including:

1. $\beta = 0 \quad (Z' = Z_\psi)$;
2. $\beta = \pi/2 \quad (Z' = Z_\chi)$;
3. $\beta = \tan^{-1}(\sqrt{3/5}) \quad (Z' = Z_\eta)$;[12]
4. $\beta = \tan^{-1}(-\sqrt{1/15}) \quad (Z' = Z_\nu)$.[13]

In addition, the Z' can mix with the Standard Model Z°. In this case, the mass of the Standard Model Z° is shifted from $M_\circ$, its SM value ($M_\circ \equiv M_W/\cos\theta_W$), as

$$M_{Z^\circ}^2 = M_\circ^2 - \tan^2\theta_E(M_{Z'}^2 - M_\circ^2),$$

where θ_E is the mixing angle and $M_{Z'}$ is the mass of the (mixed) Z'. Combining the results from CDF[14] and UA2,[15] we get $M_W = 80.6 \pm 0.4$ GeV/c^2 and the LEP experiments[9] give $\sin^2\theta_W = 0.2306 \pm 0.0004$; from these we derive $M_\circ = 91.7 \pm 0.5$ GeV/c^2, in agreement with the LEP measurement $M_{Z^\circ} = 91.16 \pm 0.03$ GeV/c^2. Thus, if a Z' exists, its mixing with the Standard Model Z° must be very small (for $M_{Z'} \sim 200$ GeV/c^2, $\tan\theta_E < 0.01$).

However, even if the Z' does not mix with the Standard Model Z°, it can mix with the photon, in which case effects of a high mass Z' might be seen at TRISTAN but not at LEP. In particular, it is interesting to note that the couplings in the Z_χ and Z_η models are such as to give destructive interference in the charged dilepton channel and an overall enhancement in the hadron channels at TRISTAN. Since, as noted above, the charged dilepton channels are measured to be somewhat low, it is not surprizing that fitting PEP/PETRA/TRISTAN results to the Z_χ and Z_η model predictions results in a finite Z' mass—for the Z_χ-model, we find a best fit for a Z_χ of mass 233^{+161}_{-32} GeV/c^2; for the Z_η model the best fit gives a Z_η of mass 144^{+80}_{-25} GeV/c^2 (see Table 1).

The finite results for the Z_χ and Z_ψ masses are provocative and lead one to examine results from other Z' searches. In particular, the CDF group has recently reported results from searches for Z's produced via the reaction

$$\bar{p}p \longrightarrow X + Z'; \quad Z' \longrightarrow e^+e^- \text{ or } \mu^+\mu^-$$

Table 1. The results of fits of various E_6-symmetry motivated Z' models to the hadron and dilepton cross sections and the forward-backward asymmetries in dilepton production, as reported by PEP/PETRA/TRISTAN experiments.

Model	Best Fit Z' Mass	Mass Limit (68% CL)
Z_ψ	$M_{Z_\psi} = \infty$	$M_{Z_\psi} > 212$ GeV/c^2
Z_χ	$M_{Z_\chi} = 233^{+161}_{-48}$ GeV/c^2	$M_{Z_\chi} > 185$ GeV/c^2
Z_η	$M_{Z_\eta} = 144^{+80}_{-25}$ GeV/c^2	$M_{Z_\eta} > 119$ GeV/c^2
Z_ν	$M_{Z_\nu} = \infty$	$M_{Z_\nu} > 214$ GeV/c^2

at a cm energy of 1.8 TeV. They report 95% c.l. lower mass limits that are in excess of 300 GeV for all of the above models, assuming that the Z's decay into known fermions.[16] The CDF result also seems to rule out the extreme case, where decays into all of the supersymmetric and exotic fermions of the E_6 model are possible, for the Z_χ and Z_η masses that come from the above-described fits. The CDF results for the $\mu^+\mu^-$ invariant mass spectrum, shown in Fig. 6, **have no hint** of a clustering near either of the two best-fit masses—where both the Z_χ– and the Z_η-model would predict some tens of events in each case.[17] Thus, if the dilepton cross section is, in fact, low, it is not easily understood in the context of existing models that contain additional heavy neutral gauge bosons.

2. Two-Photon Physics

The TRISTAN storage ring remains as the world's premier facility for the study of two-photon processes $e^+e^- \longrightarrow e^+e^- + hadrons$. As can be seen in the Feyman diagram for these processes, shown in Fig. 7, the hadrons are produced by the interaction of two virtual photons, this is the origin of the name "two-photon" processes. The characteristics of the events depends upon the degree of virtuality of the photons involved in the interaction, usually measured in terms of Q^2, the negative of the photon's squared virtual mass, which can be expressed in terms of the kinematic variables shown in Fig. 7 as $Q^2 = 4E_{tag}E_{beam}\sin^2(\Theta/2)$. For the case where both the electron and positron are scattered at small angles and are not observed in the detector ("untagged" events), the Q^2 values of the virtual photons are small and they are "quasi-real."

2.1. *Inclusive Untagged Results from AMY*

The AMY group has recently reported an analysis of untagged two-photon events seen in a 27.5 pb^{-1} data sample accumulated at center-of-mass energies ranging from 55 to 61.4 GeV. Untagged hadronic events produced by photon-photon

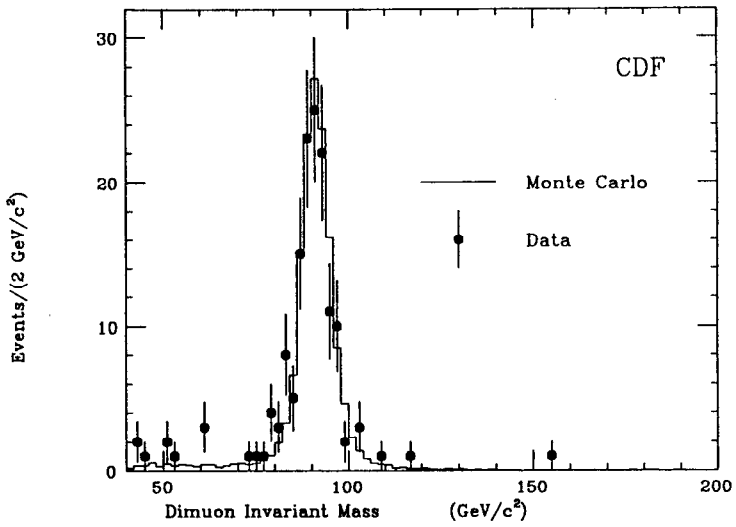

Figure 6: The invariant mass distribution for $\mu^+\mu^-$ pairs seen in the CDF detector at Fermilab.

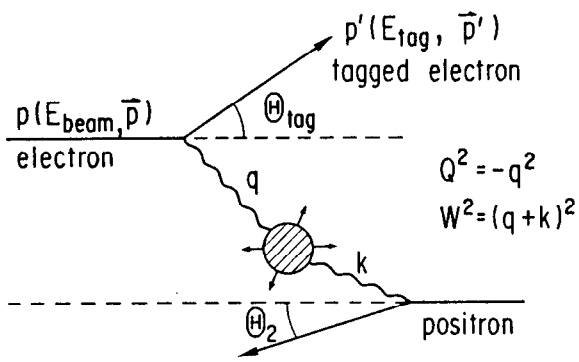

Figure 7: The Feynman diagram for the two-photon process.

interactions were selected using the following criteria:

1. The number of charged tracks with polar angle in the range $25° \leq \theta \leq 155°$ must be at least 4, and of these at least two must have momentum exceeding 0.75 GeV/c and at least one must have transverse momentum exceeding 1.0 GeV/c.

2. The most energetic cluster appearing in the calorimeter must have an energy less than $0.25E_{beam}$ (anti-tagging).

3. The net charge of the observed charged tracks must have magnitude ≤ 2.

4. The net transverse momentum $|\sum \vec{p}_{t,i}|$, where the $\vec{p}_{t,i}$ are the projections of the observed momenta on the plane transverse to the beam, must have magnitude ≤ 2.5 GeV/c.

5. The mass of the system of observed hadrons must be in the range 4 GeV/c^2 $\leq W_{vis} \leq$ 15 GeV/c^2, where the computation of W_{vis} assumes the pion mass for all charged particles.

Criterion 1 suppresses QED-type events such as $e^+e^- \longrightarrow e^+e^-\tau^+\tau^-$. Criterion 2 constrains the mass of the virtual photons to be less than about 7.5 GeV/c^2. Criteria 3 and 4 suppress beam-gas background events and poorly reconstructed events, respectively. Criterion 5 suppresses backgrounds from the one-photon annihilation process. After all background subtractions and efficiency corrections, we obtain a final count of 2703 ± 98 events. We characterize each event by the variable P_t^{jet}, where each detected particle is identified with one of two back-to-back jets, using the thrust axis to define the jet axis—the transverse momentum of each jet is defined as P_t^{jet}.

The experimental data are compared with the predictions of models for high-p_t hadron production in $\gamma\gamma$ reactions using Monte Carlo simulations. Point-like interactions of photons are modeled using a Quark Parton Model (QPM) event generator that incorporates all first-order QED radiative corrections for the process $e^+e^- \longrightarrow e^+e^-q\bar{q}$ (see Fig. 8a). The diffractive hadronic interaction of the photons is simulated by the Vector Meson Dominance (VMD) model (see Fig. 8b).

Fig. 9a shows the P_t^{jet} distribution of events with a clear excess of events over the QPM+VMD prediction (solid curve) for high P_t^{jet} values. The thrust distribution for the events with $P_t^{jet} \geq 3$ GeV/c is shown in Fig. 9b, together with the QPM+VMD prediction; it is evident that the excess is primarily due to low thrust events.

2.2. *The Multi-Jet Model for Hard Constituent Scattering*

Hard, non-diffractive hadronic interactions take place between photons when a constituent parton in one of the photons interacts with the other photon (see Fig. 10a) or one of its constituents (see Fig. 10b). These processes are expected to

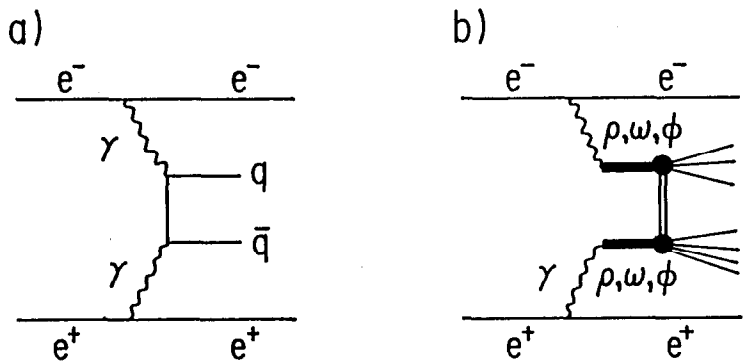

Figure 8: The lowest-order Feynman diagram for two-photon hadron production in the Quark-Parton model (a), and in the Vector-Meson-Dominance model (b).

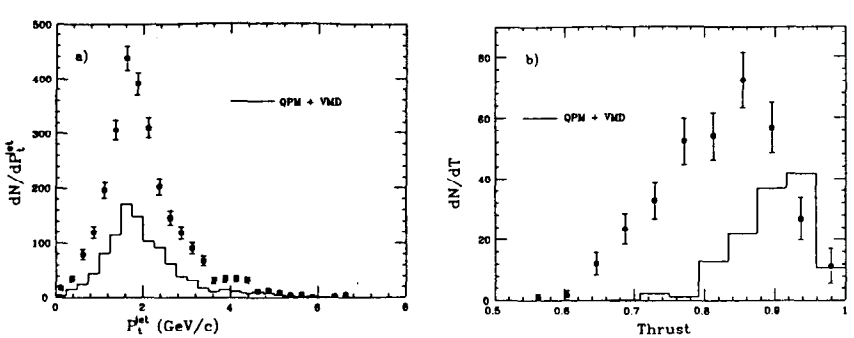

Figure 9: (a) The P_t^{jet} distribution of the selected events compared to the QPM+VMD prediction. (b) The thrust distribution for events with $P_t^{jet} \geq 3.0$ GeV/c.

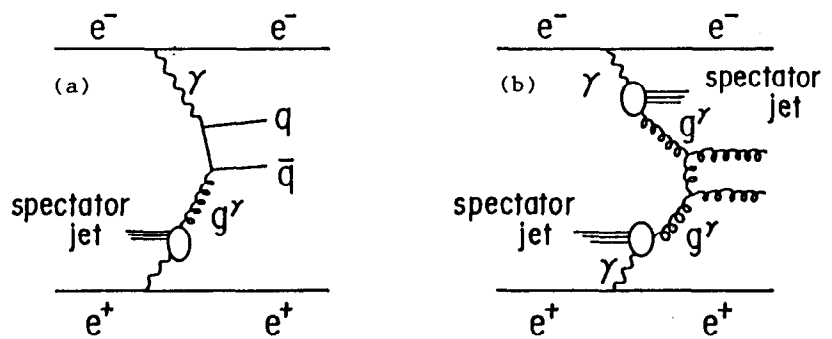

Figure 10: The lowest-order Feynman diagram for three-jet (a) and four-jet events (b) in the MJET model.

result in spectator jets of hadrons, corresponding to the remnant photon constituents, that continue along in the directions of the incident virtual photons, which are very near to the directions of the incident beam particles. Although the AMY detector's coverage for small angles is poor, Monte Carlo simulations indicate that about half of the particles in the spectator jets are detectable. Therefore, events corresponding to the processes indicated in Figs. 10a and 10b are expected to appear as events with three and four jets, respectively. These three- and four-jet events result in low-thrust event topologies. We refer to these processes as multi-jet production (MJET).

The MJET cross section for three-(four-) jet events is given by the product of the luminosity functions of two photons, parton density inside one photon (parton densities inside two photons), the subprocess cross section for the interaction between a parton and a photon (between two partons), and a kinematical factor.[18] We use the parton density given by Drees and Grassie.[19] The calculations depend on an arbitrary cutoff parameter P_t^{min}, which characterizes the minimum parton P_t used in the perturbative QCD calulation. Presumably, processes with P_t values below P_t^{min} are modeled by VMD.

Various distributions, such as those of P_t^{jet}, W_{vis}, thrust, multiplicity, and individual particle p_t , were determined using a bin-by-bin background subtraction and compared with Monte Carlo simulations. The general features of these distributions are found to be reasonably well described by the incoherent sum of QPM, VMD and

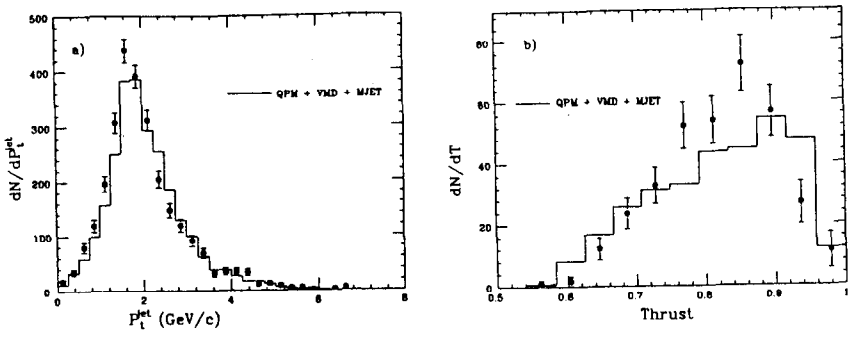

Figure 11: (a) The P_t^{jet} distribution of the selected events compared to the QPM+VMD+MJET prediction with $P_t^{min} = 1.6$ GeV/c. (b) The thrust distribution for events with $P_t^{jet} \geq 3.0$ GeV/c, compared to the QPM+VMD+MJET model.

MJET, where in the MJET model we set the cutoff parameter P_t^{min} to 1.6 GeV/c. For example, in the P_t^{jet} distribution in Fig. 11a, it can be seen that the inclusion of the hard scattering processes is enough to give a reasonably good representation of the observed data. The large excess of events over the QPM prediction at low thrust is well described by the contribution from the MJET model, as can be seen in Fig. 11b. The features of the other distributions are also reasonably well described by the incoherent sum of QPM,VMD and MJET.

2.3. Acknowledgements

I thank my colleagues at TRISTAN for providing the results reported here, and the organizers for their hard work in running this pleasant summer institute. The work at TRISTAN is supported by the Japan Ministry of Education, Science and Culture (Monbusho) and Society for the Promotion of Science, the U.S. Department of Energy and National Science Foundation, the Korean Science and Engineering Foundation and Ministry of Education, and the Academia Sinica of the People's Republic of China.

References

1. J. Fujimoto and Y. Shimizu, Mod. Phys. Lett. **A3** (1988) 581.
2. F. A. Berends, R. Kleiss, and S. Jadach, Z. Nucl. Phys. **202**, 63 (1982); Comput. Phys. Commun. **29**, 185 (1983).
3. Levan R. Surguladze and Mark A. Samuel Phys. Rev. Lett. **66**, 560 (1991); ibid, **66**, 2416E (1991). This paper pointed out an error in a previous calculation of the third-order QCD corrections by S. G. Gorishny, A.L. Kataev, and S. A. Larin, Phys. Lett. **B212**, 238 (1988), which over-estimated the effect of the $\mathcal{O}(\alpha_s^3)$ terms.
4. T. Kumita *et al.*,(AMY), Phys. Rev. **D42**, 1339 (1990). In this analysis a value of $\Lambda_{\overline{MS}} = 0.38$ GeV is derived using the incorrect $\mathcal{O}(\alpha_s^3)$ calculation noted above in ref. 3. With the newer result for the $\mathcal{O}(\alpha_s^3)$ QCD corrections, a fit yields a central value of $\Lambda_{\overline{MS}} = 0.7$ GeV.
5. J. J. Hernandez *et al.*,(Particle Data Group) Phys. Lett. **B239**, pg.III.52 (1990).
6. T. Mori *et al.*,(AMY), Phys. Lett. **B218**, 499 (1989).
7. F. Abe *et al.*,(CDF), Phys. Rev. Lett. **63**, 720 (1990).
8. G. S. Abrams *et al.*,(MARKII), Phys. Rev. Lett. 63, 2173 (1989).
9. M. Z. Akrawy *et al.*,(OPAL), Phys. Lett. **B231**, 530 (1989); D. Decamp *et al.*, (ALEPH), Phys. Lett. **B235**, 379 (1990); B. Adeva *et al.*,(L3), Phys. Lett. **B237**, 136 (1990); P. Abreu *et al.*,(DELPHI), Phys. Lett. **B241**, 435 (1990).
10. D. Haidt, Private Communication.
11. W. J. P. Beenakker, F. A. Berends and S. C. van der Marck, program ZSHAPE, Instituut Lorentz, University of Leiden (1989).
12. J. Ellis *et al.*, Mod. Phys. Lett. **11**, 57 (1986); Nucl. Phys. **B276**, 14 (1986).
13. L. E. Ibanez and J. Mas, Nucl. Phys. **B286**, 107 (1987).
14. F. Abe *et al.*,(CDF), Phys. Rev. Lett. **65**, 2243 (1990).
15. J. Alitti *et al.*,(UA2), Phys. Lett. **B241**, 150 (1990).
16. K. Maeshima (CDF), contributed talk to the Spring APS Meeting, Washington, DC (April, 1991); J. Patrick (CDF), these proceedings.
17. J. Ellis, P. J. Franzini and F. Zwirner, Phys. Lett. **B202**, 417 (1988).
18. M. Drees and R. M. Godbole, Nucl. Phys. **B339**, 355 (1990). Earlier calculations of these processes were reported by S. Brodsky *et al*, Phys. Rev. Lett. **41**, 672 (1978); Phys. Rev. **D19**, 1418 (1979), and K. Kajantie and R. Raito, Nucl. Phys. **B159**, 528 (1978).
19. M. Drees and K. Grassie, Z. Phys. **C28**, 451 (1985).